Materials Physics and Mechanics 42 (2019) 359-366 Received: April 16, 2018

MODELING PLASTIC DEFORMATION AND DAMAGE ACCUMULATION PROCESSES IN STRUCTURAL STEELS UNDER BLOCK NON-SYMMETRIC LOW-CYCLE LOADING

Ivan A. Volkov*, Leonid A. Igumnov, Denis N. Shishulin

Research Institute for Mechanics, National Research Lobachevsky State University of Nizhny Novgorod, Nizhny Novgorod, 23 Prospekt Gagarina (Gagarin Avenue) BLDG 6, 603950, Russia

*e-mail: pmptmvgavt@yandex.ru

Abstract. To assess the reliability and the scope of applicability of the defining relations of mechanics of damaged media (MDM) [1,2], plastic deformation and damage accumulation processes in a number of structural steels under low-cycle loading have been numerically investigated, and the obtained numerical results have been compared with the data from full-scale experiments. It is shown that the introduced MDM model qualitatively and quantitatively describes the main effects of plastic deformation and damage accumulation processes in structural alloys under block-type non-stationary non-symmetric low-cycle loading.

Keywords: low-cycle fatigue, plastic deformation, damage degree, block-type loading, mechanics of damaged media, modeling, numerical and full-scale experiment

1. Introduction

Many years of experimentally and theoretically studying fatigue damage accumulation in structural materials make it possible to conclude that fatigue covers the three significantly different regions of cyclic loading [3]: high-cycle fatigue (HCF), when a material works quasi-elastically, corresponding to durability values under uniaxial symmetric cyclic loading in the range of 10^5-10^8 cycles and higher; low-cycle fatigue (LCF), when a material undergoes non-stationary elastoplastic deformation, corresponding to the durability values under uniaxial symmetric cyclic loading up to 10^4 cycles; an intermediate region corresponding to the durability values of 10^4-10^5 cycles, where both the mechanisms of degradation of the initial strength properties of the material are simultaneously active.

Classical methods for predicting fatigue life using semi-empirical formulas (law) based on a stable analysis of the deformation process and connecting the parameters of loops of elastoplastic deformation with a number of cycles prior to failure require a large amount of experimental data and are valid only for a narrow range of loading conditions [1-3].

Damage and fatigue failure of structural materials is caused mainly by nucleation of microdefects, their growth and merging into macroscopic cracks. The description of the mechanical behavior of microdefects is no less important than the description of macrocrack nucleation. In the last decade a new scientific direction of mechanics of damaged media (MDM) has been successfully developed for solving such problems [1,2].

By now, a large number of constitutive relations of MDM describing damage development in a material have been developed. However, most of these equations are focused only on certain loading modes, not related to specific equations of deformation processes. In fact, the history of thermoplastic deformation (the type of strain path, the nature

http://dx.doi.org/10.18720/MPM.4232019_11

of temperature change, the type of stress state, the history of its change, etc.) significantly affects the rate of damage accumulation. This emphasizes the importance of considering the kinetics of the stress-strain state (SSS) in hazardous areas of structural elements and its theoretical description by the corresponding equations of state [1,2].

At present, approaches to evaluating fatigue life of materials and structures based on the concept of damaged media have been wildly development [1,2,4-16].

General provisions on the evolution equations of damage accumulation were formulated in [8]. It is noted that generally the strength criterion should represent a process equation rather than a boundary condition. This equation should take into account time and history (trajectory) of loading (deformation), i.e. it should be written in the speeds (increments) of the corresponding values and be closely related to the governing equations describing the process of material deformation.

In [9,10], the MDM model employed in modern computing systems of finite element analysis such as ANSYS, Abaqus, and others were elaborated. The Chaboche model consists of three interrelated parts:

- constitutive relations of cyclic plasticity;
- evolutionary equations for fatigue damage accumulation;
- strength criterion of the damaged material.

In work [5], evolutionary equation of fatigue damage accumulation for monotonic and cyclic deformation of materials is formulated on the basis of the plasticity theory with kinematic and isotropic hardening.

The process of cyclic deformation is considered to occur under soft, hard or mixed loading conditions and to be stationary or non-stationary, symmetric or asymmetric.

Work [16] presents an investigation of the processes of viscoplastic deformation and fracture of materials and structures on the basis of the composite model of the damaged material. The model is based on the ability to represent a complex process of propagation of the interrelated effects of deformation and fracture in a series of formally independent elementary acts described by respective partial models of plasticity, creep and damage accumulation. Calculation of mutual influence of such basic acts is at the top level in the general model of the damaged material.

The direct effect of damage on the deformation process is calculated in the model by introducing the dependence of elastic moduli of material on the current damage value.

The following models are used to describe the process of elastoplastic deformation and damage accumulation:

- a thermoplasticity model with a combined translational-isotropic hardening;
- a damage accumulation model based on the change in the energy of plastic deformation and on the kinetic equations for changing the damage degree at brittle fracture.

In [1,2], a mathematical model of mechanics of damaged media (MDM) was developed, describing processes of complex plastic deformation and damage accumulation in structural materials (metals and their alloys) under monotonous and cyclic proportional and non-proportional regimes of thermal-mechanical loading. In the present paper, the model is used for describing the processes in stainless steels 12X18H10T, 12X18H9 (the designation of steels in this article is given in Russian) under block-type non-stationary non-symmetric low-cycle loading. The obtained numerical results are compared with the data from full-scale experiments.

2. Defining relations of mechanics of damaged media

The damaged medium model [1,2] consists of three interrelated parts:

- the relations of elastic-plastic behavior of the material, accounting for the effect of the failure process;
- the evolutionary equations of damage accumulation kinetics;
- the strength criterion of the damaged material.

The defining relations of plasticity are based on the following basic assumptions:

- components of strain tensors e_{ij} and strain rates $\dot{e}_{ij}$ include elastic e_{ij}^e, $\dot{e}_{ij}^e$ and plastic – e_{ij}^p, $\dot{e}_{ij}^p$ strains;
- the initial yield surface for various temperatures is described by a Mises-type surface. The evolution of the yield surface is described by the evolution of its radius C_p and displacement of its center ρ_{ij};
- the body volume is elastic;
- the initial medium is isotropic. Anisotropy due to the plasticity processes is only taken into account.

In the elastic region, the correlation between the spherical and deviatoric components of the stress and strain tensors is described by Hook law.

To describe the effects of monotonous and cyclic deformation, a yield surface is introduced:

$$F_s = S_{ij}S_{ij} - C_p^2 = 0,\ S_{ij} = \sigma_{ij}^{'} - \rho_{ij}. \tag{1}$$

To describe complex cyclic deformation modes in the stress space, a cyclic "memory" surface is introduced:

$$F_p = \rho_{ij}\rho_{ij} - \rho_{\max}^2, \tag{2}$$

where $\rho_{\max}$ is maximal modulus of variable ρ_{ij} for the entire loading history.

It is assumed that the structure of the evolutionary equation for the yield surface radius has the form:

$$\dot{C} = [q_\chi H(F_\rho) + a(Q_s - C_p)\Gamma(F_\rho)]\dot{\chi} + q_3\dot{T}, \tag{3}$$

$$C_p = C_p^0 + \int_0^t \dot{C}_p dt,\ \dot{\chi} = (\frac{2}{3}\dot{e}_{ij}^p\dot{e}_{ij}^p)^{1/2},\ \chi_m = \int_0^t \dot{\chi}H(F_\rho)dt,\ \chi = \int_0^t \dot{\chi}dt, \tag{4}$$

$$q_\chi = \frac{q_2 A\psi_1 + (1-A)q_1}{A\psi_1 + (1-A)},\ Q_s = \frac{Q_2 A\psi_2 + (1-A)Q_1}{A\psi_2 + (1-A)},\ 0 \le \psi_i \le 1,\ i = 1,2$$

$$A = 1 - cos^2\theta, cos\,\theta = n_{ij}^e n_{ij}^s, n_{ij}^e = \frac{\dot{e}_{ij}'}{(\dot{e}_{ij}'\dot{e}_{ij}')^{1/2}}, n_{ij}^s = \frac{S_{ij}}{(S_{ij}S_{ij})^{1/2}},$$

$$H(F_\rho) = \begin{Bmatrix} 1, F_\rho = 0 \wedge \rho_{ij}\dot{\rho}_{ij} > 0 \\ 0, F_\rho < 0 \vee \rho_{ij}\dot{\rho}_{ij} \le 0 \end{Bmatrix}, \Gamma(F_\rho) = 1 - H(F_\rho), \tag{5}$$

where q_1, q_2, q_3 are isotropic hardening moduli, Q_1 and Q_2 are cyclic hardening moduli, a is a constant defining the stabilization process rate of the hysteresis loop of cyclic deformation of the material, Q_s is stationary value of the yield surface radius for the $\rho_{\max}$ and T, C_p^0 is initial value of the yield surface radius.

$$\dot{\rho}_{ij} = \tilde{g}_1\dot{e}_{ij}^p - g_2\rho_{ij}\dot{\chi} + \dot{\rho}_{ij}^*,\ \rho_{ij} = \int_0^t \dot{\rho}_{ij}dt, \tag{6}$$

$$\tilde{g}_1 = g_1 + k_1\left(1 - e^{-k_2\chi_m}\right)\langle\cos\beta\rangle,\ \rho_{ij} = \int_0^t \dot{\rho}_{ij}dt, \tag{7}$$

$$\dot{\rho}_{ij}^{*} = g_3 \dot{e}_{ij}^{p} H\left(F_\rho\right) - g_4 \rho_{ij} \dot{\chi}\,, \tag{8}$$

where g_1, g_2, g_3, g_4, k_1 и k_2 are experimentally determined material parameters.

For non-symmetric both hard and soft cyclic loading, term $\dot{\rho}_{ij}^{*}$ enables equation (6) to describe the processes of placing and ratcheting of the cyclic plastic hysteresis loop. For $g_3 = g_4 = k_1 = 0$, one obtains from (6) a special case of equation (6) – the Armstrong–Frederick–Kadashevich equation:

$$\dot{\rho}_{ij} = g_1 \dot{e}_{ij}^{p} - g_2 \rho_{ij} \dot{\chi}\,. \tag{9}$$

To describe the evolution of the "memory" surface, it is necessary to formulate an equation for $\rho_{\max}$:

$$\dot{\rho}_{\max} = \frac{(\rho_{ij}\dot{\rho}_{ij})H(F_\rho)}{(\rho_{mn}\rho_{mn})^{1/2}} - g_2 \rho_{\max} \dot{\chi} - g_3 \rho_{\max} \dot{T}\,. \tag{10}$$

The plastic strain rate tensor components obey the law of orthogonality of the plastic strain rate vector to the yield surface at the loading point:

$$\dot{e}_{ij}^{p} = \lambda S_{ij}\,. \tag{11}$$

At the stage of the development of defects scattered over the bulk, the effect of damage on the physical-mechanical properties of the material is observed. This effect can be accounted for by introducing effective stresses:

$$\tilde{\sigma}'_{ij} = F_1(\omega)\sigma'_{ij} = \frac{G}{\tilde{G}}\sigma'_{ij} = \frac{\sigma'_{ij}}{(1-\omega)\left[1 - \dfrac{(6K+12G)}{(9K+8G)}\omega\right]},$$

$$\tilde{\sigma} = F_2(\omega)\sigma = \frac{K}{\tilde{K}}\sigma = \frac{\sigma}{4G(1-\omega)/(4G+3K\omega)},\ \tilde{\rho}_{ij} = F_1(\omega)\rho_{ij}\,, \tag{12}$$

where $\tilde{G}$, $\tilde{K}$ are effective moduli of elasticity determined using McKenzie formulae [2,6].

It is postulated that the rate of the damage accumulation process for low-cycle fatigue (LCF) is defined by an evolutionary equation of the form [1,2,7,8]:

$$\dot{\omega} = f_1(\beta)\, f_2(\omega)\, f_3(W)\, f_4\left(\dot{W}\right), \tag{13}$$

where functions f_i, i=1…4 account for: capacity of stressed state ($f_1(\beta)$), level of accumulated damage ($f_2(\omega)$), accumulated relative damage energy for the nucleation of defects ($f_3(W)$) and rate of change of damage energy ($f_4\left(\dot{W}\right)$).

In equation (13):

$$f_1(\beta) = \exp(\beta),\ f_2(\omega) = \begin{cases} \omega^{1/3}(1-\omega)^{2/3} \wedge W > W_a \wedge \omega \le 1/3, \\ \dfrac{\sqrt[3]{16}}{9}\omega^{-1/3}(1-\omega)^{-2/3} \wedge W > W_a \wedge \omega > 1/3, \end{cases} \tag{14}$$

$$\dot{\omega} = f_1(\beta)\, f_2(\omega)\, f_3(W)\, f_4\left(\dot{W}\right), \tag{15}$$

where β is capacity parameter of stressed state ($\beta = \sigma/\sigma_u$), W_a is value of the damage energy at the end of the nucleation stage of scattered defects under LCF, and W_f is energy value corresponding to the formation of a macroscopic crack.

The condition when damage level ω reaches its critical value

$$\omega = \omega_f \le 1 \tag{16}$$

is taken as a criterion of the termination of the phase of the development of scattered micro-defects.

3. Numerical results

Specimens of 12X18H10T stainless steel were experimentally tested in the conditions of hard uniaxial tension-compression at ambient temperature. The testing program consisted of five blocks including monotonous and cyclic loading [5]:

- the first block consists of 20 cycles of symmetric hard cyclic loading with the strain amplitude of e_{11}=0.0008;
- the second block implements monotonous tension up to e_{11}=0.05;
- the third block consists of 200 cycles of non-symmetric cyclic loading with the strain range of $\Delta e_{11} = e_{11}^{(+)} - e_{11}^{(-)}$=0.012 and average strain $e_{11}^{(m)}$=0.044 (during this block, placing of the plastic hysteresis loop takes place);
- in the fourth block, monotonous tension up to e_{11}=0.01 is realized;
- the fifth block implements non-symmetric cyclic loading with the strain range of $\Delta e_{11} = e_{11}^{(+)} - e_{11}^{(-)}$=0.012 and average strain $e_{11}^{(m)}$=0.094 up to failure (number of cycles to failure N_f=2800). During this loading block, placing of the plastic hysteresis loop also takes place.

Tables 1–3 list the main physical-mechanical parameters of the MDM model for steel 12X18H10T, determined from the results of the basic experiment [1,2], which are used in the calculations.

Table 1. Physical-mechanical characteristics and parameters of the MDM model

K, MPa	G, MPa	C_p^o, MPa	g_1, MPa	g_2	g_3, MPa	g_4	k_1, MPa	k_2	a
165277	76282	203	20850	297	660	3	10000	0.2	5

Table 2. Modulus of cyclic hardening $Q_S(\rho_{\max})$ (MPa)

Q_S, MPa	203	210	232	232	232	232	232
$P_{\max}$, MPa	0	30	60	90	100	110	120

Table 3. Modulus of monotonous hardening q_χ (MPa)

q_k, MPa	-17000	-4634	-811	371	737	849
χ	0	0.002	0.004	0.006	0.008	0.01

q_k, MPa	897	900	900	900	900	900	900
χ	0.015	0.02	0.03	0.04	0.05	0.09	0.15

Figure 1 depicts the 20-th cycle of symmetric loading followed by monotonous tension up to $e_{11} = 0.05$ and the first cycle of non-symmetric loading. Here and in what follows the dots correspond to the test data and the solid lines show the computational results.

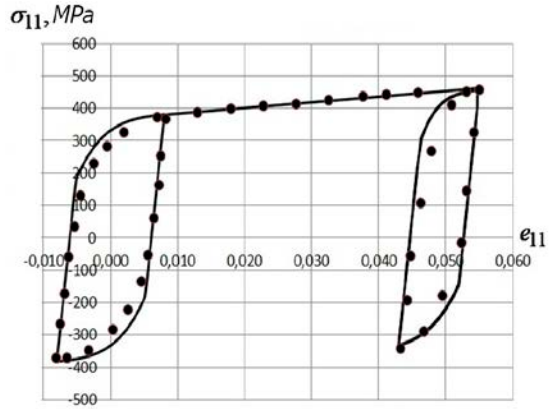

Fig. 1. Deformation diagram during the transition from symmetric cyclic loading to asymmetrical cyclic loading by monotonic stretching

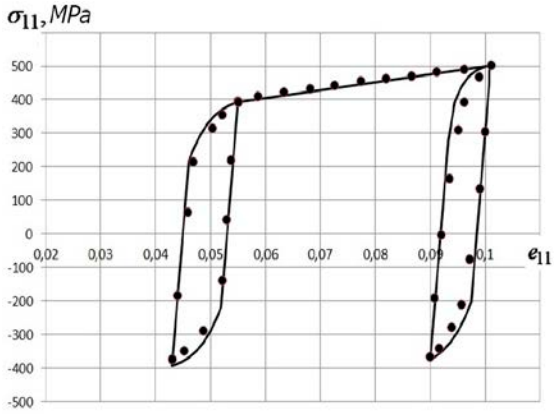

Fig. 2. Deformation diagram during the transition from the third to the fifth block of asymmetric cyclic loading

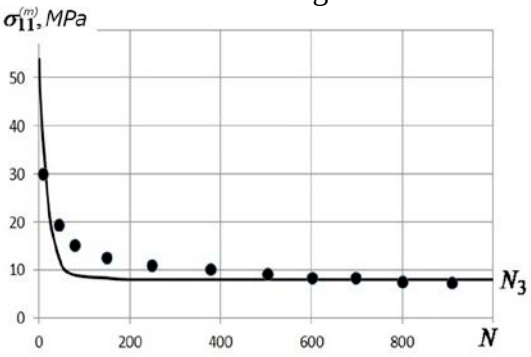

Fig. 3. The dependence of the average stress in the cycle on the number of cycles for the third block of loading

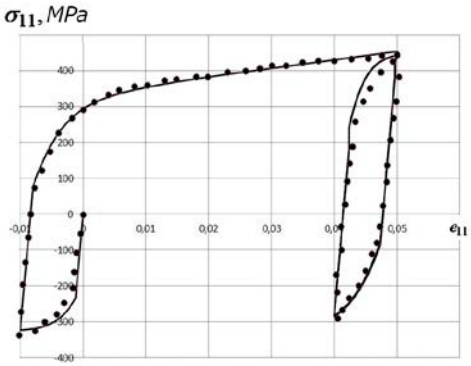

Fig. 4. Deformation process for the second loading block

Figure 2 shows the cyclic deformation diagram at the end of the third (the 200-th cycle) and the beginning of the fifth (the 1-st cycle) loading blocks. Figure 3 presents the results illustrating the processes of placing of the plastic hysteresis loop during the third block of non-symmetric cyclic loading (variation of the average stress $\sigma_{11}^{(m)}$ over the cycle in the process of cyclic loading). Both qualitative and quantitative agreement of the experimental and computational data is observed.

Specimens of stainless steel 12X18H9 were experimentally studied under hard non-stationary non-symmetric cyclic loading consisting of two blocks:

- in the first block, the specimen is compressed up to the strain of e_{11}=0.01, followed by tension up to e_{11}=0.05;
- in the second block, non-symmetric hard cyclic loading with the strain range of $\Delta e_{11} = e_{11}^{(+)} - e_{11}^{(-)}$=0.01 is implemented up to failure (N_f=850). Here, placing of the plastic hysteresis loop tales place (Fig. 5), and after the 500-th loading cycle the loop becomes practically symmetric;

Tables 4–6 list the main physical-mechanical characteristics and material parameters of the MDM model for steel 12X18H9 as determined from the results of the basic experiment [1,2], which are used in the calculations.

Table 4. Physical-mechanical characteristics and parameters of the MDM model

K, MPa	G, MPa	C_p^o, MPa	g_1, MPa	g_2	g_3, MPa	g_4	k_1, MPa	k_2	a	W_a, J/m^3	W_f, MJ/m^3
165277	76282	190	24090	286	800	2	10000	0.2	5	0	800

Table 5. Modulus of cyclic hardening $Q_S(\rho_{\max})$ (MPa)

Q_S, MPa	190	205	210	215	220	225	225
$P_{\max}$, MPa	0	20	40	60	80	100	120

Table 6. Modulus of monotonous hardening q_χ (MPa)

q_χ, MPa	-5000	-4471	-4188	-3859	-2460	-182
χ	0	0.002	0.004	0.006	0.008	0.01

q_χ, MPa	888	1531	1274	913	913	913
χ	0.015	0.02	0.03	0.04	0.05	0.06

Figure 4 shows the deformation process for steel 12X18H9 during the second loading block (500-th cycle).

Figure 5 depicts the history of average stress $\sigma_{11}^{(m)}$ over a cycle in the process of cyclic loading during the second block. Both qualitative and quantitative agreement of the experimental and numerical results is also observed.

Figure 6 presents a fatigue curve for stainless steel 12X18H9 under hard symmetric cyclic loading. The comparison of the experimental and computational results testifies to their qualitative and, adequate for engineering design purposes, quantitative agreement.

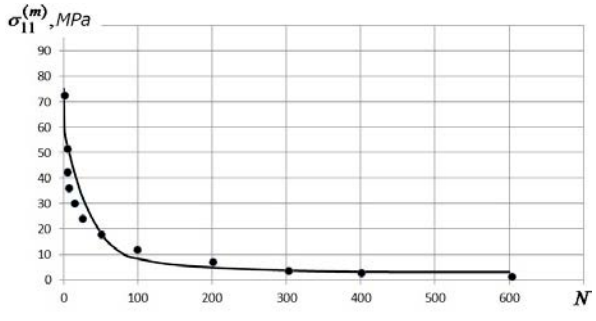

Fig. 5. The dependence of the average stress in the cycle on the number of cycles for the second loading block

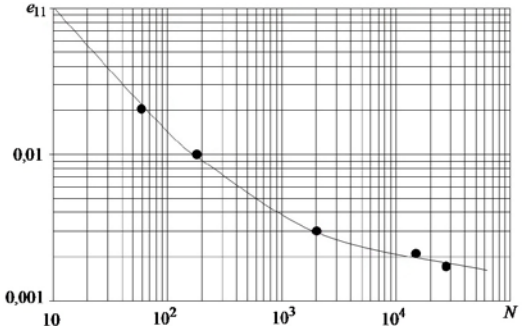

Fig. 6. Fatigue curve for steel 12X18H9

Inverse Fourier transform, sine and cosine transformation are done numerically through an algorithm presented in [12,13].

4. Conclusion

The comparison of the results of numerical experiments against the test data on plastic deformation and damage accumulation in stainless steels (12X18H10T, 12X18H9) under block non-stationary non-symmetric low-cycle loading corroborates the reliability of the defining equations of the MDM model and its adequacy in determining material parameters.

This result are in addition to the results obtained earlier in [11-13,15] when were considered problems of constructing surface Green's functions.

Acknowledgements. *The work is financially supported by the Federal Targeted Program for Research and Development in Priority Areas of Development of the Russian Scientific and Technological Complex for 2014-2020 under the contract No. 14.578.21.0246 (unique identifier RFMEFI57817X0246).*

References

[1] Volkov IA, Korotkikh YG. *Equations of state of viscoelastoplastic damaged media.* Moscow: Fizmatlit; 2008. (In Russian)
[2]Volkov IA, Igumnov LA. *Introduction to continuum mechanics damaged enviroment.* Moscow: Fizmatlit; 2017. (In Russian)
[3] Collins J. *Renormalization.* Moscow: Mir; 1984.
[4] Lemaitre J. Damage modelling for prediction of plastic or creep fatigue failure in structures. In: *Trans. 5th Int. Conf. SMRiT*. North Holland; 1979. p.L 5/1b.
[5] Bondar VS, Abashe DR, Petrov VK. Comparative analysis of variants of plasticity theories under cyclic loading. *PNRPU Mechanics Bulletin.* 2017;2: 23-44. (In Russian)
[6] Murakami S. Deformation damage theory of materials and its application to the analysis of the deformation process of square plates. *J. Mec. Theor. Appl.* 1982;1: 743-761.
[7] Bonder SR, Lindholm US. The criteria of the growth of defects for time-dependent failure of materials. *Proc. Amer. Soc. Mech. Eng. Ser. D. Theoret. Bases of Eng. Calculations.* 1976;100(2): 51-58. (In Russian)
[8] Lemaitre J. A continuum model of damage used in analyzing failure of plastic materials. *Proc. Amer. Soc. Mech. Eng. Ser. D Theoret. Bases of Eng. Calculations.* 1985;107(1): 90-98. (In Russian)
[9] Chaboche JL. Constitutive equation for cyclic plasticity and cyclic viscoplasticity. *Inter. J. of Plasticity*. 1989;5(3): 247-302.
[10] Chaboche JL. Continuous damage mechanics a tool to describe phenomena before crack initiation. *Engineering Design.* 1981;64(2): 233-247.
[11] Cardebois JP, Sidoroff F. Damage Induced Elastic Anisotropy. In: Boehler JP. (ed.) *Mechanical Behavior of Anisotropic Solids / Comportment Méchanique des Solides Anisotropes.* Dordrecht: Springer; 1982. p.761-774.
[12] Betten J. Damage tensors in continuum mechanics. *Journal de Mechanigue et appligue.* 1983;2(1): 13-32.
[13] Beaver PW. Biaxial Fatigue and Fracture of Metals: a Review. *Metals Forum.* 1985;8(1): 14-29.
[14] Jordan EU, Broun MW, Miller KJ. Fatique under severe nonproportional loading. In: *ASTM STP 853*. Philadelphia: American Soc. for Testing and Material; 1985. p.569–585.
[15] Wang J, Chaw CL. Mixed mode ductile fracture studies with nonproportional loading bazed on continuum damage mechanics. *Trans. ASME. J. Eng. Mater. and Technolog*. 1989;111(2): 204-209.
[16] Kapustin SA, Churilov YA, Gorokhov VA. *Modelirovanie nelineynogo modelirovaniya i razrusheniya konstruktsiy v usloviyakh mnogofaktornykh vozdeystviy na osnove MKE.* Nyzhny Novgorod: Izdatelstvo NNGU; 2015. (In Russian)